

RESEARCH ARTICLE | OCTOBER 01 2024

Moiré photonic superlattice-induced transparency at commensurate angle in a terahertz metasurface composed of triple layer square lattices

Xuelian Zhang ; Zhenyu Zhao  ; Rajour Tanyi Ako; Sharath Sriram ; Xuan Zhao; Hongxin Liu; Haijun Bu  



Appl. Phys. Lett. 125, 141701 (2024)

<https://doi.org/10.1063/5.0229684>



Articles You May Be Interested In

On-chip light trapping in bilayer moiré photonic crystal slabs

Appl. Phys. Lett. (December 2022)

Molecular orientation and lattice ordering of C₆₀ molecules on the polar FeO/Pt(111) surface

J. Chem. Phys. (January 2012)

Synthetic gauge fields and Landau levels in acoustic Moiré superlattices

Appl. Phys. Lett. (July 2023)

08 October 2024 01:10:55

Nanotechnology & Materials Science

Optics & Photonics

Impedance Analysis

Scanning Probe Microscopy

Sensors

Failure Analysis & Semiconductors



Unlock the Full Spectrum.
From DC to 8.5 GHz.

Your Application. Measured.

[Find out more](#)



Moiré photonic superlattice-induced transparency at commensurate angle in a terahertz metasurface composed of triple layer square lattices

Cite as: Appl. Phys. Lett. **125**, 141701 (2024); doi: [10.1063/5.0229684](https://doi.org/10.1063/5.0229684)

Submitted: 18 July 2024 · Accepted: 24 September 2024 ·

Published Online: 1 October 2024



View Online



Export Citation



CrossMark

Xuelian Zhang,¹ Zhenyu Zhao,^{1,a)} Rajour Tanyi Ako,² Sharath Sriram,² Xuan Zhao,³ Hongxin Liu,³ and Haijun Bu^{3,a)}

AFFILIATIONS

¹Department of Physics, Shanghai Normal University, Shanghai 200234, China

²Functional Materials and Microsystems Research Group and the Micro Nano Research Facility, and the ARC Centre of Excellence for Transformative Meta-Optical Systems, RMIT University, Melbourne, VIC 3000, Australia

³Suzhou Institute of Metrology, Suzhou 215163, China

^{a)}Authors to whom correspondence should be addressed: zyzhao@shnu.edu.cn and buhj@szjl.com.cn

ABSTRACT

The control of the speed of terahertz waves is always a challenge since the bandgap of most optical materials is much larger beyond meV with subtle nonlinear susceptibility. Moiré metasurfaces are shown to exhibit wide tunable optical properties and extraordinary physical phenomena at specific commensurate angles. These can be achieved by a careful design of the metasurface to manipulate terahertz slow light. Herein, we demonstrate a triple layer Moiré metasurface with a distinct electromagnetically induced transparency (EIT) phenomenon at commensurate angles. The proposed metasurface is composed of an intrinsic square lattice embedded into another Moiré photonic superlattice made of twisted square lattice at commensurate angles of 10.39° and 7.63° . The coupling between adjacent meta-atoms on the combined metasurface leads to destructive interference of dual trapped lattice modes, which results in a transparency window at the terahertz band. A maximum group delay of 9.76 ps is found at the transparent window of 0.84 THz when the commensurate angle is 10.39° . When the commensurate angle reduces to 7.63° , the transparency window shifts to 0.57 THz with a 5.96 ps group delay. The coupled Lorentz oscillator model indicates that the nonlinear optical susceptibility at transparency windows is above zero. Our results create an approach to tune the EIT as well as slow light in the terahertz band. Our device can have potential applications in terahertz signal processing and storage.

Published under an exclusive license by AIP Publishing. <https://doi.org/10.1063/5.0229684>

Moiré superlattice is a structure of interference by two or more overlapping periodic lattices of identical nano-flakes of two-dimensional (2D) materials.¹ They exhibit extraordinary phenomena for potential application in optoelectronics and photonics, such as Moiré lasers,² Moiré polaritons,^{3,4} Moiré excitons/trions,^{5–8} hybridized excitons,^{9,10} symmetry-breaking optoelectronics,^{11,12} infrared photo-response,^{13–15} etc. However, to date, the functional area of above-mentioned devices is limited to flake-size of 2D materials at hundreds of millimeters. An alternative approach is using artificial Moiré metasurface^{16–19} to control photons by twisting the photonic lattice at specific angles. This can have wide application, including the control of group velocity of surface plasmon,²⁰ localization of photonic states,²¹ bound states in the continuum,²² flat photonic band,^{2,23} etc. These optical features can be precisely manipulated by tuning the twisted angles between two photonic lattices. Thus, a large-scale functional

area of photonic device with high tunability can be realized. Furthermore, Moiré metasurfaces have abundant photonic responses than their periodic counterparts owing to the quasi-periodicity of Moiré fringes.

Electromagnetically induced transparency (EIT) is a phenomenon of significant interest in modern photonics, particularly for its applications in slow light and quantum information processing.^{24–26} Traditionally, EIT has been achieved through the complex layout of sub-wavelength resonators, such as split-ring resonators (SRRs), cut-wires, and U-shaped resonators, which rely on the interplay between super-radiative and sub-radiative resonators to create the necessary quantum interference.^{27–30} However, this approach requires precise design and calibration, limiting the system's practical flexibility. Moiré photonic superlattices offer an alternative approach because of their highly tunable optical characteristics. By simply adjusting the

commensurate angle of the Moiré fringes, the electromagnetic response can be tuned, simplifying the design process and enabling extraordinary optical phenomena. It not only eliminates the need for complex resonator designs but also offers significant potential for developing advanced photonic devices. However, EIT phenomena have never been reported in Moiré photonic superlattices.

In this work, we demonstrate a unique EIT phenomenon in a Moiré metasurface at commensurate angles, termed Moiré photonic superlattice-induced transparency (MPSIT). Such a Moiré metasurface is composed of a triple layer square lattice, of which the first and the second layers twisted at a specific angle results in a photonic superlattice with Moiré fringes. Such a specific angle is termed as commensurate angle. In this work, we investigate the analytical and numerical insight

into the evolution of the MPSIT windows as well as the variation of slow light phenomenon. Furthermore, the nonlinear susceptibility of the Moiré metasurface is calculated, and the detailed analysis is discussed.

We propose a Moiré metasurface of twisted square photonic lattice. The meta-atoms (MAs) on lattice-site are made of metallic disks. The principle of quasi-periodic fringes of Moiré photonic superlattice is illustrated in Fig. 1(a). First, a bilayer Moiré metasurface is constructed by superimposing two initial square photonic lattices with a combined commensurate angle of 2θ , shown in Fig. 1. The first layer of square photonic lattice is twisted anti-clockwise with a half commensurate angle of θ while the second layer of square lattice is twisted clockwise with half commensurate angle of θ . The radius of metallic

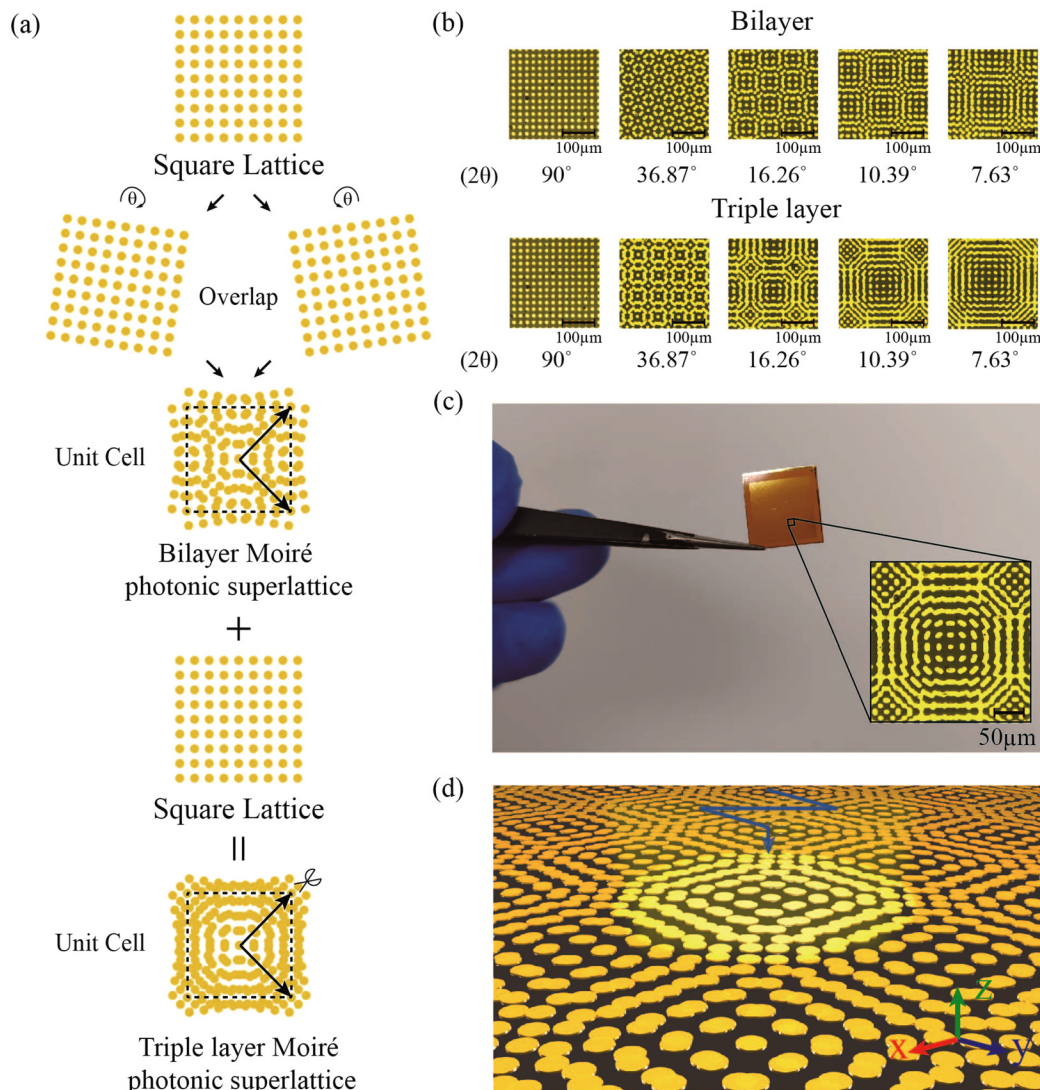


FIG. 1. (a) Schematic of initial square lattice and corresponding Moiré fringes. The circular dots indicate the gold MAs. θ : commensurate angle, dash-area: unit cell. (b) Microscopic images of Moiré metasurfaces composed of bilayer (upper) and triple layer square lattice (lower) samples at different commensurate angles. (c) The photograph of the entire Moiré metasurface sample. The inset shows a microscopically enlarged image of the sample of the Moiré metasurface composed of a triple layer square lattice at the angle of 10.39° . (d) Schematic diagram showing terahertz wave through the Moiré metasurface.

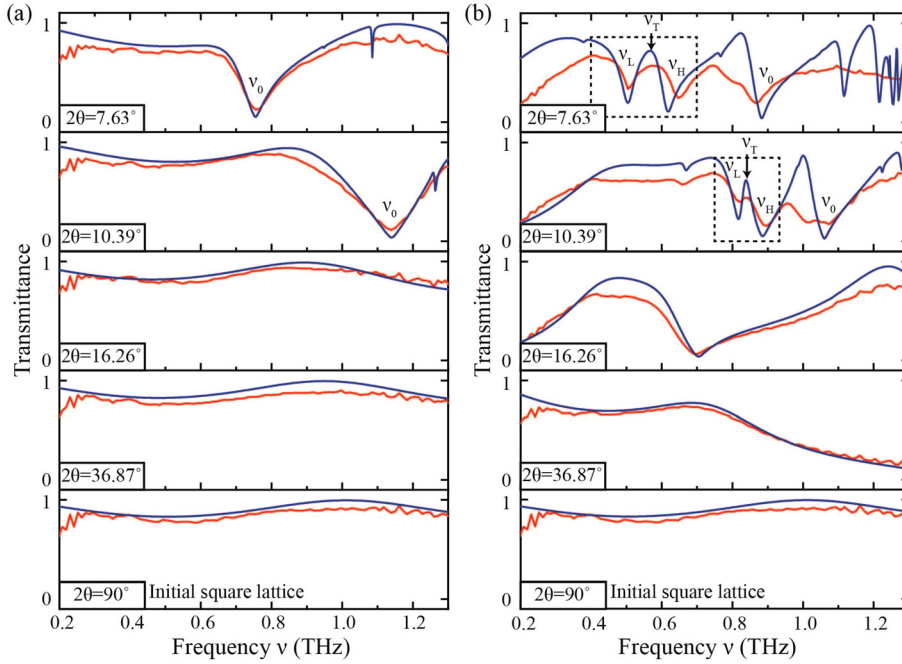


FIG. 2. Transmittance spectra of Moiré metasurfaces composed of bilayer (a) and triple layer (b) square photonic lattice at different commensurate angles. Red line: measurement; blue line: simulation. The dash rectangles indicate the coupling regions of MPSIT effect.

TABLE I. The simulated values of resonance frequency of each mode and the transparent windows.

Design (2θ)	Bilayer	Triple layer			
	ν_0 (THz)	ν_0 (THz)	ν_L (THz)	ν_T (THz)	ν_H (THz)
7.63°	0.75	0.88	0.50	0.57	0.62
10.39°	1.14	1.06	0.82	0.84	0.89

MAs is $R = 6 \mu\text{m}$, and the spacing between the two neighboring MAs is $8 \mu\text{m}$. Correspondingly, the period of square lattice is $L = 20 \mu\text{m}$. The metal thickness of all MAs is identical to $0.2 \mu\text{m}$. Additionally, a third layer of square lattice is overlapped on the Moiré photonic superlattice, resulting in a triple layer Moiré metasurface. The details about the derivation of commensurate angles are presented in our [supplementary material](#).

The fringes of the Moiré photonic superlattice at commensurate angles leads to a quasi-periodicity L_m , which is related to the twisted angle between the two layers of square lattice as follows:^{31–33}

$$L_m = \frac{L}{\sin(\theta)}, \quad (1)$$

TABLE II. The fitting parameters of coupled Lorentz oscillators.

Commensurate angle	A	B	κ	ω (THz)	γ_1 (THz)	γ_2 (THz)	ω_1 (THz)	ω_2 (THz)
7.63°	2.21	1.164	1.43	0.99	0.42	0.49	3.26	3.87
10.39°	3.3	6.66	3.87	0.87	0.13	0.84	4.89	5.25

where L is the lattice constant of the initial square lattice. Moreover, the commensurate angle 2θ and m value satisfy the following relation:

$$2\theta = 2 \sin^{-1} \left(\frac{1}{\sqrt{(2m-1)^2 + 1}} \right), \quad m = 1, 2, 3, 4, \dots, \quad (2)$$

where m is a positive integer. Here, we focus on several commensurate angles for twisted square lattice, as is determined by $m = 2, 4, 6, 8$, respectively. The Moiré photonic superlattice has the commensurate angles 2θ of $36.87^\circ, 16.26^\circ, 10.39^\circ$, and 7.63° . The fringes of the Moiré photonic superlattice will be degenerated to intrinsic photonic lattice at a commensurate angle $2\theta = 90^\circ$, owing to the C_{4v} symmetry of intrinsic photonic lattice. The quasi-periodicities of corresponding Moiré photonic superlattices are $L_m = 63.25, 141.42, 220.91$, and $300.67 \mu\text{m}$. Here, the trilayer Moiré metasurface has the same quasi-periodicity as the bilayer Moiré metasurface. [Figure 1\(b\)](#) presents the microscopic images of Moiré metasurfaces composed of bilayer and triple layer square lattice samples at different commensurate angles, and the photograph of the entire sample of Moiré metasurface is illustrated in [Fig. 1\(c\)](#). A small commensurate angle induces a large photonic superlattice. When the third layer of square lattice is introduced into the Moiré photonic superlattice, its fringes become aperiodic at commensurate angles. The simulations of the terahertz transmittance of metasurface are obtained by the frequency-domain solver of CST

Microwave StudioTM platform. Figure 1(d) shows a schematic of the metasurface incident normally with terahertz waves. The details about the simulation, fabrication, and characterization of the Moiré metasurface can be found in the [supplementary material](#).

Figure 2 presents the simulated and measured transmittance of the Moiré metasurfaces as a function of frequency. The transmittances of Moiré metasurfaces composed of bilayer square photonic lattice are shown in Fig. 2(a). There are no intrinsic resonances to the single-layer metasurface of intrinsic photonic lattice as well as the Moiré metasurface at commensurate angles of $2\theta = 36.87^\circ$ and 16.26° , respectively, in Fig. 2. However, a resonance mode on the metasurface with commensurate angles $2\theta = 10.39^\circ$ and 7.63° show a broad linewidth labeled as ν_0 . This broad resonance mode shows a redshift as the commensurate angle decreases from 10.39° to 7.63° . This

phenomenon is consistent with our previous work,³⁴ which confirms that the larger the m number, the smaller the twisted angle θ , and the lower resonance frequency ν_0 of superlattice modes. The superlattice mode is out of our frequency range for the case of commensurate angle $2\theta = 36.87^\circ$ and 16.26° . Upon introduction of the third intrinsic square lattice onto the Moiré photonic superlattice, the resonance mode, ν_0 , shifts red slightly. Figure 2(b) shows an EIT phenomenon between ν_L and ν_H at commensurate angles $2\theta = 10.39^\circ$ and 7.63° . The details of the superlattice mode as well as the induced transparency windows are listed in Table I.

Here, ν_T refers to the central frequency of the EIT window, ν_H and ν_L refers to the higher frequency and lower frequency resonance dips crossing the induced transparency windows. Since ν_T exhibits a lower frequency than the superlattice mode ν_0 , it cannot be the

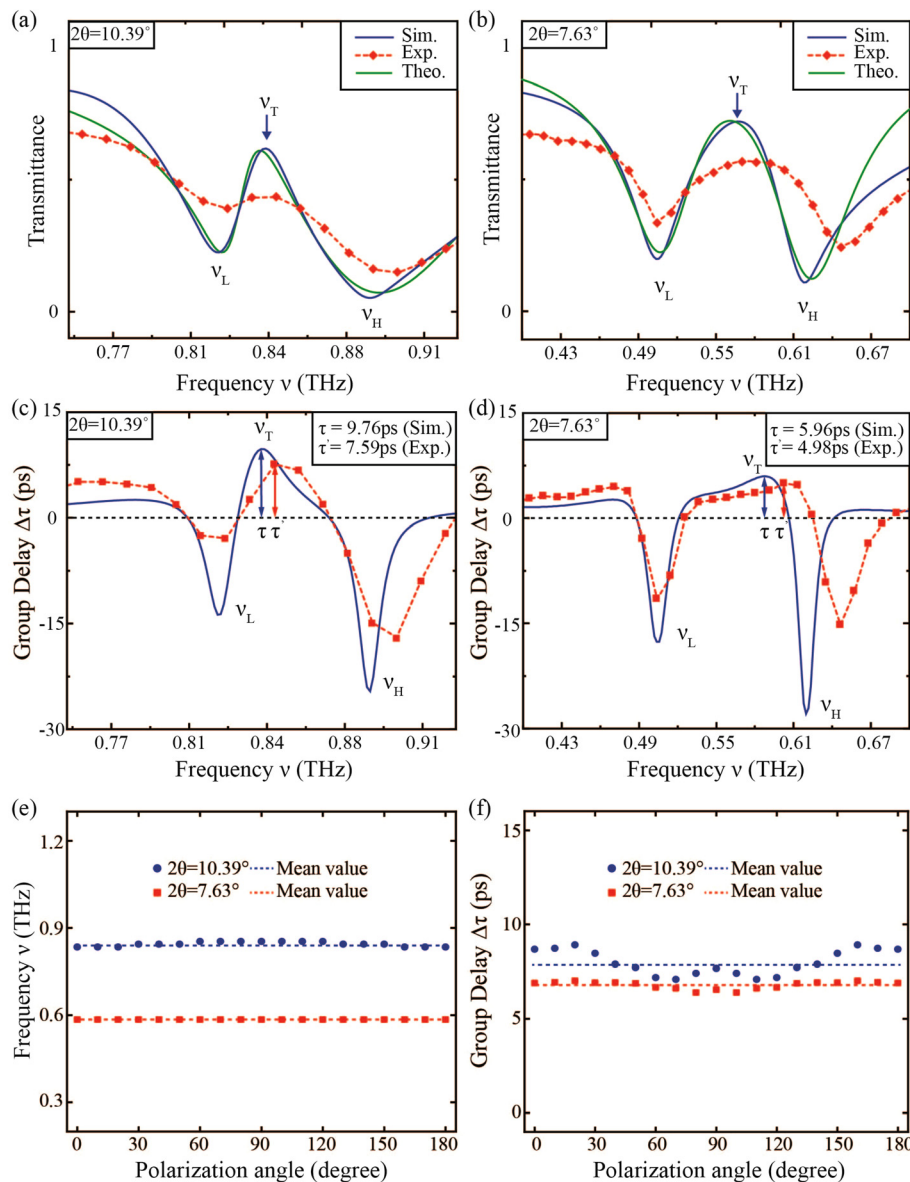


FIG. 3. (a) The transmittances of the coupled region of the MPSIT effect of the Moiré metasurface composed of a triple layer square photonic lattice at a commensurate angle $2\theta = 10.39^\circ$. (b) The transmittances of the coupled region of the MPSIT effect of the Moiré metasurface composed of a triple layer square photonic lattice at a commensurate angle $2\theta = 7.63^\circ$. (c) Group delay of the MPSIT effect of the Moiré metasurface composed of a triple layer square photonic lattice at a commensurate angle $2\theta = 10.39^\circ$. (d) Group delay of the MPSIT effect of the Moiré metasurface composed of a triple layer square photonic lattice at a commensurate angle $2\theta = 7.63^\circ$. The experimentally measured frequency (e) and group delay (f) as a function of polarization angle based on Moiré metasurfaces composed of a triple layer square photonic lattice, respectively.

destructive interference of the photonic superlattice mode itself. Actually, the third layer square lattice inserted into the existing Moiré superlattice will cause a complex trapped lattice mode coupling. Thus, the first layer lattice and the second lattice interplay with the third layer square lattice at half commensurate angle $\pm\theta$. The mirror symmetry of the above-mentioned two-body interaction must lead to dual trapped lattice modes correspondingly, which is expected to interfere destructively, once again. Thus, it results in the aforementioned MPSIT phenomenon. The deviation between simulated and experimental results is mainly due to precision limitations in our manufacturing process and the low spectral resolution of the THz-TDS (9.6 GHz).

To reveal the underlying physics of the MPSIT phenomenon, we use the coupled Lorentz oscillators (CLO) model to mimic the behavior of MPSIT effects on the Moiré metasurfaces composed of a triple layer square photonic lattice in the terahertz transmission spectrum. The equations can be written as^{35,36}

$$\frac{d^2 x_1(t)}{dt^2} + \gamma_1 \frac{dx_1(t)}{dt} + \omega_1^2 x_1(t) + \kappa^2 x_2(t) = \frac{QE}{M}, \quad (3)$$

$$\frac{d^2 x_2(t)}{dt^2} + \gamma_2 \frac{dx_2(t)}{dt} + \omega_2^2 x_2(t) + \kappa^2 x_1(t) = \frac{qE}{m}. \quad (4)$$

Herein, the two trapped lattice modes are designated as oscillators 1 and 2, respectively. (Q, q) , (M, m) , (ω_1, ω_2) , and (γ_1, γ_2) are the effective charges, effective masses, resonance angular frequencies, and the loss factors of the oscillators. κ defines the coupling strength of the two trapped lattice modes. Here, we consider that both oscillators interact with the incident THz electric field $E = E_0 e^{i\omega t}$. In the above-mentioned coupled equations, we substitute $q = Q/A$ and $m = M/B$, where A and B are dimensionless constants that dictate the relative coupling of incoming radiation with the oscillators. Now by expressing the

displacement vectors for oscillators 1 and 2 as $x_1 = c_1 e^{i\omega t}$ and $x_2 = c_2 e^{i\omega t}$, we solve the above-mentioned coupled equations (3) and (4) for x_1 and x_2 as follows:

$$x_1 = \frac{\frac{B}{A}\kappa^2 + (\omega^2 - \omega_2^2 + i\omega\gamma_2)}{\kappa^4 - (\omega^2 - \omega_1^2 + i\omega\gamma_1)(\omega^2 - \omega_2^2 + i\omega\gamma_2)} \frac{Q}{M} E_0, \quad (5)$$

$$x_2 = \frac{\kappa^2 + \frac{B}{A}(\omega^2 - \omega_1^2 + i\omega\gamma_1)}{\kappa^4 - (\omega^2 - \omega_1^2 + i\omega\gamma_1)(\omega^2 - \omega_2^2 + i\omega\gamma_2)} \frac{Q}{M} E_0. \quad (6)$$

The CLO models fitting results are listed in Table II. The coupling coefficient κ determines the coherence of the collective resonance between the photonic lattices, which shapes the spectral configuration of the induced transparency window.

Obviously, the fitting results exhibit good agreement with the corresponding experimentally measured and numerically simulated curves of MPSIT windows, as shown in Figs. 3(a) and 3(b).

Another remarkable character of MPSIT effects is the presentation of a group delay ($\Delta\tau$) at the transparency window in the frequency spectrum. Here, $\Delta\tau$ represents the time delay of the terahertz wave packet instead of the group index. $\Delta\tau$ can be calculated by the following equation:

$$\Delta\tau = -\frac{d\varphi}{2\pi d\nu}, \quad (7)$$

where φ and ν refer to the effective phase and frequency of the terahertz complex transmission spectrum, respectively. The measured group delay $\Delta\tau$ achieves 8 and 5 ps at commensurate angle 2θ , corresponding to 10.39° and 7.63° , respectively. However, the simulated group delay at commensurate angles 10.39° and 7.63° is 9.76 and 5.96

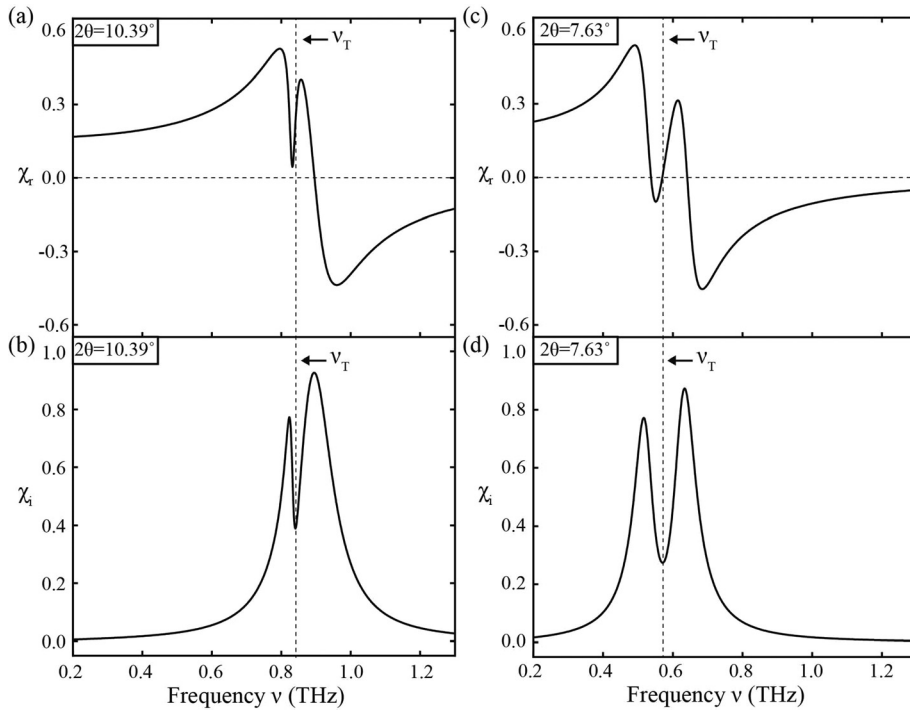


FIG. 4. (a) The real part of electric susceptibility as a function of the frequency of the Moiré metasurface composed of a triple layer square photonic lattice at a commensurate angle $2\theta = 10.39^\circ$. (b) The imaginary part of electric susceptibility as a function of the frequency of the Moiré metasurface composed of a triple layer square photonic lattice at a commensurate angle $2\theta = 10.39^\circ$. (c) The real part of electric susceptibility as a function of the frequency of the Moiré metasurface composed of a triple layer square photonic lattice at a commensurate angle $2\theta = 7.63^\circ$. (d) The imaginary part of electric susceptibility as a function of the frequency of the Moiré metasurface composed of a triple layer square photonic lattice at a commensurate angle $2\theta = 7.63^\circ$.

ps, respectively. In Figs. 3(c) and 3(d), there are minor differences between the numerical model and the experimental measurement. It could be associated with small imperfections in the fabrication process. In addition, the experimentally measured frequency and group delay as a function of polarization angle is shown in Figs. 3(e) and 3(f), respectively. The chosen polarization angle for the experimental test changes every 10° . Both the measured frequency at induced transparency window and its corresponding group delay exhibit minor fluctuations with the theoretical value. This confirms that the MPSIT is polarization independent due to the C_4 symmetry of square photonic lattice.

Actually, the group velocity is subject to the dielectric dispersion, which is determined by the electric susceptibility written as $\chi = \chi_r + i\chi_i$. The susceptibility χ , which relates the polarization, P , of the oscillator to the strength of incoming electric field, E , is then expressed in terms of the displacement vectors as^{35,36}

$$\chi = \frac{P}{\epsilon_0 E} = \frac{Qx_1 + qx_2}{\epsilon_0 E}, \quad (8)$$

$$\chi = \frac{K}{A^2 B} \left(\frac{A(B+1)\kappa^2 + A^2((\omega^2 - \omega_2^2) + B(\omega^2 - \omega_1^2))}{\kappa^4 - (\omega^2 - \omega_1^2 + i\omega\gamma_1)(\omega^2 - \omega_2^2 + i\omega\gamma_2)} + i\omega \frac{A^2\gamma_1 + B\gamma_2}{\kappa^4 - (\omega^2 - \omega_1^2 + i\omega\gamma_1)(\omega^2 - \omega_2^2 + i\omega\gamma_2)} \right), \quad (9)$$

where K refers to the coefficient used to fit the CLO model. As shown in Figs. 4(a) and 4(c), the real part of the susceptibility disappears closely at ν_T . Since the second-order derivative of χ_r is close to zero, there is negligible dispersion in group velocity, and a pulse centered at the transparency frequency passes through the medium without distortion. Figures 4(b) and 4(d) show the imaginary part of the susceptibility is above zero, leading to energy dissipation at the terahertz band. From Eq. (9), the real part of the susceptibility is inversely proportional to the square of the coupling coefficient (κ). In other words, as the coupling strength between the layers increase, the susceptibility decreases, which in turn leads to a greater group delay at the transparency windows. This inverse proportionality provides evidence that the observed

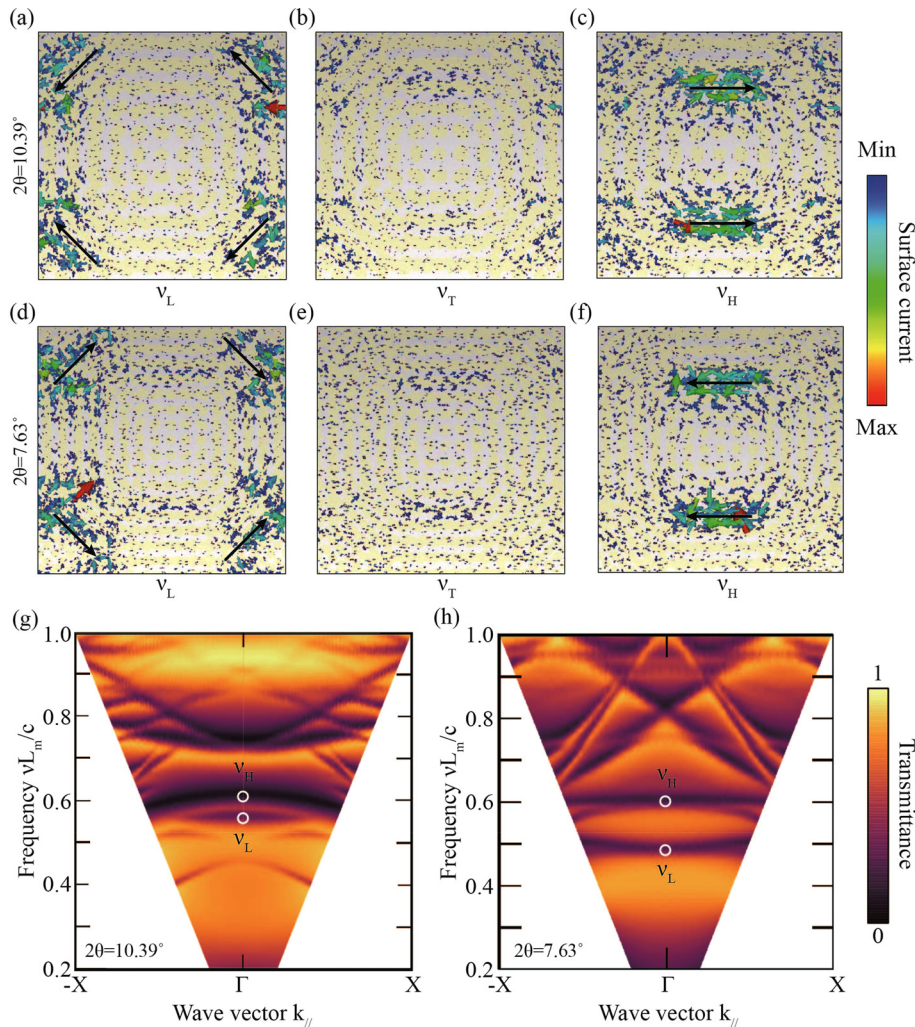


FIG. 5. (a)–(f) Simulated surface current distribution of the resonance mode and transparent windows at the MPSIT region of a triple layer square photonic lattice at commensurate angles $2\theta = 10.39^\circ$ (upper panel) and 7.63° (lower panel). The black arrows indicate the main flow direction of the surface current in the high-density region. Transmittances of Moiré metasurfaces composed of a triple layer square photonic lattice at commensurate angles $2\theta = 10.39^\circ$ (g) and 7.63° (h) under TM excitation as a function of frequency and in-plane wave vector. The frequency is normalized to c/L_m .

group delay at the transparency windows is a direct result of the trapped lattice mode coupling.

Furthermore, the simulated surface currents on the metasurface show a one-directional current flow along the edge of each Moiré fringe. This is depicted by two resonance dips of the MPSIT windows, as shown in Figs. 5(a)–5(f). The surface plasmons propagating along the metallic spacing between the disks are a manifestation of an electron density wave, which is driven by the electric component of incident terahertz wave. As shown in Figs. 5(a)–5(f), two pairs of tilted dipoles result in the resonance dip of ν_L , while a pair of parallel dipoles results in the resonance dip of ν_H . The current direction of ν_L and ν_H is opposite to each other. As such, the destructive interference of ν_L and ν_H almost vanishes at ν_T , resulting in a transparent window appearing at commensurate angles of 10.39° and 7.63° .

The photonic band structure of as-proposed Moiré metasurfaces is calculated at commensurate angles $2\theta = 10.39^\circ$ and 7.63° under the TM mode, as shown in Figs. 5(g) and 5(h). Here, $k_{//}$ is the in-plane wave vector and c is the speed of light in vacuum. The white circles shown in Figs. 5(g) and 5(h) are used to denote ν_L and ν_H at commensurate angles $2\theta = 10.39^\circ$ and 7.63° . Obviously, there is no photonic flatband between the mode of ν_L and ν_H in the space near the Γ point. Normally, the slope of the photonic band with respect to $k_{//}$ is relatively flat near the Γ point at the bottom of the photonic bandgap. This indicates that the group velocity of wave package achieves zero. However, our MPSIT phenomenon is different from the other slow light behavior induced by photonic flatband. Herein, we valued trapped lattice mode coupling of Moiré photonic superlattices composed of multiple layer square lattices.

In summary, we have experimentally and numerically investigated the terahertz MPSIT effect in the Moiré metasurface composed of twisted square photonic lattice in mirror symmetry. A symmetric twisted bilayer square lattice leads to a Moiré fringe with only distinct photonic superlattice modes ν_0 at commensurate angles of 10.39° and 7.63° . Furthermore, a third layer square photonic lattice is inserted onto a double layer Moiré photonic superlattice. This leads to a destructive interference of trapped lattice modes. The resulting metasurface gives rise to photonic superlattice-induced transparency phenomenon. A maximum group delay of 9.76 ps is found at the transparent window of 0.84 THz when the commensurate angle achieves 10.39° . When the commensurate angle reduces to 7.63° , the transparency windows shift to 0.57 THz with a 5.96 ps group delay. The coupled Lorentz model study indicates that the nonlinear optical susceptibility at transparency windows is non-zero. The real part of the susceptibility disappears at the aforementioned transparency frequency, and the imaginary part of the susceptibility is above zero, leading to an energy dissipation medium in the terahertz band. The surface current distribution indicates that the destructive interference of trapped lattice modes gives rise to a transparency window at ν_T . Finally, the photonic band structure shows no flatband near the Γ point at the frequency of the MPSIT windows. Our results manifest an approach to achieve tunable slow light in the terahertz band. This is significant for signal processing and storage in the terahertz band.

See the [supplementary material](#) for the experimental details of simulation, fabrication, and characterization of Moiré metasurface. The mathematical deviation of commensurate angles of the Moiré metasurface is listed as well.

This work was performed in part at the Micro Nano Research Facility at RMIT University in the Victorian Node of the Australian National Fabrication Facility (ANFF).

This work was funded by the National Natural Science Foundation of China (No. 62475159) and the Science and Technology Program of Jiangsu Administration for Market Regulation (No. KJ2024021).

AUTHOR DECLARATIONS

Conflict of Interest

The authors have no conflicts to disclose.

Author Contributions

Xuelian Zhang and Zhenyu Zhao contributed equally to this work.

Xuelian Zhang: Data curation (equal); Formal analysis (equal); Investigation (equal); Methodology (equal); Validation (equal); Writing – original draft (equal); Writing – review & editing (equal). **Zhenyu Zhao:** Conceptualization (equal); Funding acquisition (equal); Investigation (equal); Supervision (equal); Writing – original draft (equal); Writing – review & editing (equal). **Rajour Tanyi Ako:** Investigation (equal); Resources (equal); Validation (equal); Writing – review & editing (equal). **Sharath Sriram:** Project administration (equal); Resources (equal); Supervision (equal); Validation (equal). **Xuan Zhao:** Funding acquisition (equal). **Hongxin Liu:** Resources (equal). **Haijun Bu:** Funding acquisition (equal); Resources (equal).

DATA AVAILABILITY

The data that support the findings of this study are available within the article and its [supplementary material](#).

REFERENCES

- 1L. Du, M. R. Molas, Z. Huang, G. Zhang, F. Wang, and Z. Sun, “Moiré photonics and optoelectronics,” *Science* **379**(6639), eadg0014 (2023).
- 2X.-R. Mao, Z.-K. Shao, H.-Y. Luan, S.-L. Wang, and R.-M. Ma, “Magic-angle lasers in nanostructured moiré superlattice,” *Nat. Nanotechnol.* **16**(10), 1099–1105 (2021).
- 3D. N. Basov, M. M. Fogler, and F. J. García De Abajo, “Polaritons in van der Waals materials,” *Science* **354**(6309), aag1992 (2016).
- 4L. Zhang, F. Wu, S. Hou, Z. Zhang, Y.-H. Chou, K. Watanabe, T. Taniguchi, S. R. Forrester, and H. Deng, “Van der Waals heterostructure polaritons with moiré-induced nonlinearity,” *Nature* **591**(7848), 61–65 (2021).
- 5K. Tran, G. Moody, F. Wu, X. Lu, J. Choi, K. Kim, A. Rai, D. A. Sanchez, J. Quan, A. Singh, J. Embley, A. Zepeda, M. Campbell, T. Autry, T. Taniguchi, K. Watanabe, N. Lu, S. K. Banerjee, K. L. Silverman, S. Kim, E. Tutuc, L. Yang, A. H. MacDonald, and X. Li, “Evidence for moiré excitons in van der Waals heterostructures,” *Nature* **567**(7746), 71–75 (2019).
- 6C. Jin, E. C. Regan, A. Yan, M. Iqbal Bakti Utama, D. Wang, S. Zhao, Y. Qin, S. Yang, Z. Zheng, S. Shi, K. Watanabe, T. Taniguchi, S. Tongay, A. Zettl, and F. Wang, “Observation of moiré excitons in WSe_2/WS_2 heterostructure superlattices,” *Nature* **567**(7746), 76–80 (2019).
- 7E. Liu, E. Barré, J. Van Baren, M. Wilson, T. Taniguchi, K. Watanabe, Y.-T. Cui, N. M. Gabor, T. F. Heinz, Y.-C. Chang, and C. H. Lui, “Signatures of moiré trions in $WSe_2/MoSe_2$ heterobilayers,” *Nature* **594**(7861), 46–50 (2021).
- 8K. L. Seyler, P. Rivera, H. Yu, N. P. Wilson, E. L. Ray, D. G. Mandrus, J. Yan, W. Yao, and X. Xu, “Signatures of moiré-trapped valley excitons in $MoSe_2/WSe_2$ heterobilayers,” *Nature* **567**(7746), 66–70 (2019).
- 9E. M. Alexeev, D. A. Ruiz-Tijerina, M. Danovich, M. J. Hamer, D. J. Terry, P. K. Nayak, S. Ahn, S. Pak, J. Lee, J. I. Sohn, M. R. Molas, M. Koperski, K. Watanabe, T. Taniguchi, K. S. Novoselov, R. V. Gorbachev, H. S. Shin, V. I.

- Fal'ko, and A. I. Tartakovskii, "Resonantly hybridized excitons in moiré superlattices in van der Waals heterostructures," *Nature* **567**(7746), 81–86 (2019).
- ¹⁰Y. Tang, J. Gu, S. Liu, K. Watanabe, T. Taniguchi, J. Hone, K. F. Mak, and J. Shan, "Tuning layer-hybridized moiré excitons by the quantum-confined Stark effect," *Nat. Nanotechnol.* **16**(1), 52–57 (2021).
- ¹¹Q. H. Wang, K. Kalantar-Zadeh, A. Kis, J. N. Coleman, and M. S. Strano, "Electronics and optoelectronics of two-dimensional transition metal dichalcogenides," *Nat. Nanotechnol.* **7**(11), 699–712 (2012).
- ¹²C. Ma, S. Yuan, P. Cheung, K. Watanabe, T. Taniguchi, F. Zhang, and F. Xia, "Intelligent infrared sensing enabled by tunable moiré quantum geometry," *Nature* **604**(7905), 266–272 (2022).
- ¹³G. Chen, A. L. Sharpe, P. Gallagher, I. T. Rosen, E. J. Fox, L. Jiang, B. Lyu, H. Li, K. Watanabe, T. Taniguchi, J. Jung, Z. Shi, D. Goldhaber-Gordon, Y. Zhang, and F. Wang, "Signatures of tunable superconductivity in a trilayer graphene moiré superlattice," *Nature* **572**(7768), 215–219 (2019).
- ¹⁴J. Yang, G. Chen, T. Han, Q. Zhang, Y.-H. Zhang, L. Jiang, B. Lyu, H. Li, K. Watanabe, T. Taniguchi, Z. Shi, T. Senthil, Y. Zhang, F. Wang, and L. Ju, "Spectroscopy signatures of electron correlations in a trilayer graphene/hBN moiré superlattice," *Science* **375**(6586), 1295–1299 (2022).
- ¹⁵B. Deng, C. Ma, Q. Wang, S. Yuan, K. Watanabe, T. Taniguchi, F. Zhang, and F. Xia, "Strong mid-infrared photoresponse in small-twist-angle bilayer graphene," *Nat. Photonics* **14**(9), 549–553 (2020).
- ¹⁶G. Hu, A. Krasnok, Y. Mazor, C.-W. Qiu, and A. Alù, "Moiré hyperbolic metasurfaces," *Nano Lett.* **20**(5), 3217–3224 (2020).
- ¹⁷Z. Wu and Y. Zheng, "Moiré metamaterials and metasurfaces," *Adv. Opt. Mater.* **6**(3), 1701057 (2018).
- ¹⁸S. Liu, S. Ma, R. Shao, L. Zhang, T. Yan, Q. Ma, S. Zhang, and T. J. Cui, "Moiré metasurfaces for dynamic beamforming," *Sci. Adv.* **8**(33), eabo1511 (2022).
- ¹⁹H. Li, D. Wang, G. Xu, K. Liu, T. Zhang, J. Li, G. Tao, S. Yang, Y. Lu, R. Hu, S. Lin, Y. Li, and C.-W. Qiu, "Twisted moiré conductive thermal metasurface," *Nat. Commun.* **15**(1), 2169 (2024).
- ²⁰E. Karademir, S. Balci, C. Kocabas, and A. Aydinli, "Lasing in a slow plasmon moiré cavity," *ACS Photonics* **2**(7), 805–809 (2015).
- ²¹P. Wang, Y. Zheng, X. Chen, C. Huang, Y. V. Kartashov, L. Torner, V. V. Konotop, and F. Ye, "Localization and delocalization of light in photonic moiré lattices," *Nature* **577**(7788), 42–46 (2020).
- ²²L. Huang, W. Zhang, and X. Zhang, "Moiré quasibound states in the continuum," *Phys. Rev. Lett.* **128**(25), 253901 (2022).
- ²³A. Kocabas, S. S. Senlik, and A. Aydinli, "Slowing down surface plasmons on a Moiré surface," *Phys. Rev. Lett.* **102**(6), 063901 (2009).
- ²⁴A. H. Safavi-Naeini, T. Alegre, J. Chan, M. Eichenfield, M. Winger, Q. Lin, J. T. Hill, D. E. Chang, and O. Painter, "Electromagnetically induced transparency and slow light with optomechanics," *Nature* **472**, 69–73 (2011).
- ²⁵M. Manjappa, S. Chiam, L. Cong, A. A. Bettiol, W. Zhang, and R. Singh, "Tailoring the slow light behavior in terahertz metasurfaces," *Appl. Phys. Lett.* **106**, 181101 (2015).
- ²⁶R. Singh, I. A. I. Al-Naib, Y. Yang, D. R. Chowdhury, W. Cao, C. Rockstuhl, T. Ozaki, R. Morandotti, and W. Zhang, "Observing metamaterial induced transparency in individual Fano resonators with broken symmetry," *Appl. Phys. Lett.* **99**, 201107 (2011).
- ²⁷Z. Zhao, H. Zhao, R. T. Ako, S. Nickl, and S. Sriram, "Polarization-insensitive terahertz spoof localized surface plasmon-induced transparency based on lattice rotational symmetry," *Appl. Phys. Lett.* **117**, 011105 (2020).
- ²⁸Z. Zhao, Z. Gu, R. T. Ako, H. Zhao, and S. Sriram, "Coherently controllable terahertz plasmon-induced transparency using a coupled Fano-Lorentzian metasurface," *Opt. Express* **28**(10), 15573–15586 (2020).
- ²⁹Z. Zhao, H. Zhao, R. T. Ako, J. Zhang, H. Zhao, and S. Sriram, "Demonstration of group delay above 40 ps at terahertz plasmon-induced transparency windows," *Opt. Express* **27**, 26459–26470 (2019).
- ³⁰Z. Zhao, X. Zheng, W. Peng, J. Zhang, H. Zhao, Z. Luo, and W. Shi, "Localized terahertz electromagnetically-induced transparency-like phenomenon in a conductively coupled trimer metamolecule," *Opt. Express* **25**(20), 24410–24424 (2017).
- ³¹C. Huang, F. Ye, X. Chen, Y. V. Kartashov, V. V. Konotop, and L. Torner, "Localization-delocalization wavepacket transition in Pythagorean aperiodic potentials," *Sci. Rep.* **6**(1), 32546 (2016).
- ³²H. Tang, B. Lou, F. Du, M. Zhang, X. Ni, W. Xu, R. Jin, S. Fan, and E. Mazur, "Experimental probe of twist angle-dependent band structure of on-chip optical bilayer photonic crystal," *Sci. Adv.* **9**(28), eadh8498 (2023).
- ³³J.-H. Han, I. Kim, J.-W. Ryu, J. Kim, J.-H. Cho, G.-S. Yim, H.-S. Park, B. Min, and M. Choi, "Rotationally reconfigurable metamaterials based on moiré phenomenon," *Opt. Express* **23**(13), 17443 (2015).
- ³⁴L. Wang, Z. Zhao, R. T. Ako, and S. Sriram, "Terahertz superlattice modes in moiré metasurface composed of twisted square and hexagonal lattices," *Appl. Phys. Express* **14**(6), 062003 (2021).
- ³⁵R. Yahiaoui, M. Manjappa, Y. K. Srivastava, and R. Singh, "Active control and switching of broadband electromagnetically induced transparency in symmetric metadevices," *Appl. Phys. Lett.* **111**(2), 021101 (2017).
- ³⁶F.-Y. Meng, Q. Wu, D. Erni, K. Wu, and J.-C. Lee, "Polarization-independent metamaterial analog of electromagnetically induced transparency for a refractive-index-based sensor," *IEEE Trans. Microwave Theory Tech.* **60**(10), 3013–3022 (2012).